Effective thermal conductivity of composite: Numerical and experimental study

M. Karkri[1*]
[1]Université Paris Est Créteil Van de Marne, CERTES, 61 avenue du Général de Gaulle, 94010 Créteil Cedex, France
* Corresponding author: mustapha.karkri@u-pec.fr

Abstract: In this paper, thermal properties of composites are investigated numerically and experimentally. In the numerical study, finite-elements method is used to modelize heat transfer and to calculate the Effective Thermal Conductivity (*ETC*) of the composite for three elementary cells, such as simple cubic (*SC*), body centered cubic (*BCC*) and face centered cubic (*FCC*). The effect of the filler concentrations, the ratio of thermal conductivities of filler to matrix material and the Kapitza resistance of the contact inclusion/matrix on the effective conductivity was investigated. A periodical method was used to measure simultaneously thermal conductivity, specific heat and diffusivity of the composite consisting of epoxy resin matrix filled with brass spheres. A comparison between the numerically calculated thermal conductivities, measured and analytical ones for various samples is made and the significance of the findings will be discussed in the paper.

Keywords: Thermal properties, Composite materials, Finite elements method, Analytical models, Inverse problem.

1. Introduction

The knowledge of the effective thermal conductivity of composites is becoming increasingly important in many engineering application and in technological developments. Numerous theoretical and empirical models have been proposed to predict the effective thermal conductivity [1-4]. Numerous numerical studies of thermal conductivity of filled polymer were conducted in the past. Deissler's [5] works were extended by Wakao and Kato [6] for a cubic or orthorhombic array of uniform spheres in contact. Shonnard and Whitaker [7] have investigated the influence of contacts on two-dimensional models. They have developed a global equation with an integral method for heat transfer in the medium. Auriault and Ene [8] have investigated the influence of the interfacial thermal barrier on the effective conductivity and on the structure of the macroscopic heat transfer equations. Using the finite elements method, Veyret at al. [9] studied the heat conductive transfer in the periodic distribution of the filler in the composite materials. In their study, calculation was carried out on two and three-dimensional geometric spaces. The same method was used by Ramani and Vaidyanathan [10] that have incorporated the effect of microstructural characteristics such as filler aspect ratio, interfacial thermal resistance, volume fraction, and filler dispersion to determine the effective thermal conductivity of a composite with spherical and parallelepipedic fillers. The thermal conductivity has increased from $0.32\,W.m^{-1}K^{-1}$ for pure PA6 to $2.09\,W.m^{-1}K^{-1}$ for spherical copper powder filler with a 50% volume fraction. A numerical approach to calculate the *ETC* of granular reinforced composite was proposed by Cruz [11]. Many other contributing works were attributed to Yin et al. [12], Kumlutas et al. [13] and Jiang et al. [14]. Recently, *ANSYS* software was used by Liang [15], to perform the numerical simulation of the heat-transfer process in hollow-glass-bead (HGB)-filled polymer composites. The effects of the content and size of the HGB on the effective thermal conductivity was identified. The effective thermal conductivity of the polypropylene (PP)/HGB composites was estimated at temperatures varying from 25 to 30 °C. Lattice Monte Carlo (*LMC*) and finite element analyses were used on the *ETC* of sintered metallic hollow spheres structures, Fiedler et al. [16]. In their work, the *LMC* calculation strategy is enhanced in order to incorporate temperature dependence of thermal conductivity and specific heat in transient thermal analyses [17]. In this paper, the effective thermal conductivity of brass spheres/resin epoxy is investigated numerically and

experimentally. The ETC was calculated using the *COMSOL* software. The obtained values are compared with experimental results and some existing theoretical and semi-empirical models.

2. Prediction methods of effective thermal conductivity

2.1. Mathematical modeling and Finite Element Solution.

Using the finite-element software *COMSOL* 3.5b, thermal analysis was carried out for the three-dimensional conductive heat transfer. About the geometry, we considered three unit cells corresponding to some arrangements such as simple cubic (*SC*), body centered cubic (*BCC*) and face centered cubic (*FCC*). The simple cubic body is composed of a sphere of radius r centered in a cubic cavity of dimensions $(2\times b)^3$ (Figure 1).

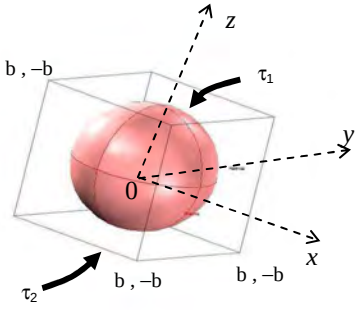

Figure 1. Simple cubic body.

The heat transfer in the elementary cell is governed by the stationary heat transfer equations. At the interphase the temperature potential jumps across the interface. The associated normal component of the heat flux is continuous and is proportional to the jump in temperature potential. The boundary conditions at the edges of the elementary cell are of adiabatic type except at the upper and lower faces where temperature is prescribed with σ and τ the filler and the matrix temperatures respectively and r_c the thermal contact resistance. According to the symmetries, only one-sixteenth of the original simple cubic cell needs to be meshed (Fig. 2). The mathematical equations representing the heat transfer model are given by the equations system (1-7).

Matrix :

$$\nabla(\lambda_m \nabla\tau) = 0 \quad (1)$$

$$\tau = \tau_1 \ , \ z = +b \ \text{ and } \ \tau = \tau_2 \, , z = -b \quad (2)$$

$$\tau = (\tau_1 + \tau_2)/2 \ , \ z = 0 \quad (3)$$

$$\lambda_m \frac{\partial\tau}{\partial n} = (\sigma - \tau)/r_c \, , \text{ matrix } \cap \text{ sphere} \quad (4)$$

$$-\lambda_m \frac{\partial\tau}{\partial n} = 0, \ \text{ lateral faces} \quad (5)$$

Sphere :

$$\nabla(\lambda_f \nabla\sigma) = 0 \quad (6)$$

$$-\lambda_f \frac{\partial\sigma}{\partial n} = (\tau - \sigma)/r_c \ \text{ sphere} \cap \text{ matrix} \quad (7)$$

Where n is the normal unit vector pointing from the filler to the matrix**.** In order to simplify the problem and to decrease the computing time, dimensionless parameters and variables were used:

$X = x/r$, $Y = y/r$ and $Z = z/r$: the dimensionless space variables.

$S = (2\sigma - \tau_1 - \tau_2)/(\tau_1 - \tau_2)$: the unknown inner temperatures field.

$T = (2\tau - \tau_1 - \tau_2)/(\tau_1 - \tau_2)$: the unknown outer temperatures field. $B = (2b - 2r)/2r$: the reduced resistance of the matrix layer between nearest spheres. $D = \lambda_m / \lambda_f$ is the conductivity ratio between the two phases. $C = r_c\lambda_m / r$ is the reduced contact resistance located at the sphere interface.

$E = \lambda_{eff} / \lambda_m$: the effective thermal conductivity.

The effective thermal conductivity E is calculated versus four parameters (the relative thermal contact resistance between particle and matrix *C*, the half distance between the particles divided by the sphere radius *B*, the filler volume fraction ϕ and the ratio of thermal conductivity between the two phases *D)*. In order to obtain high accuracy for the *ETC* computation with each model (*SC*, *BCC* and *FCC*), the refinement mesh around small geometrical features and on the upper face ($z = b$) was considered (Fig. 2). In the light of a previous work [18], the effective thermal conductivity for each model is calculated versus the heat flux crossing the elementary cells.

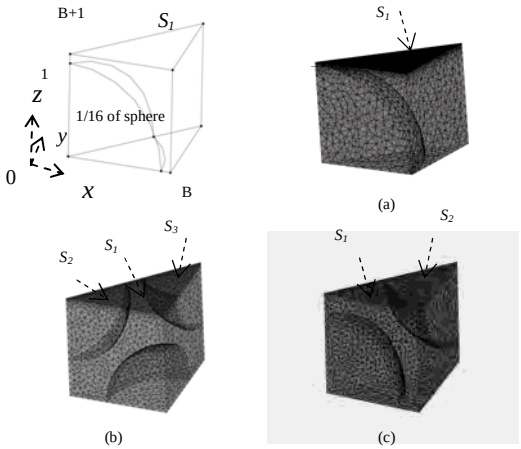

Figure 2: Mesh of elementary cell for SC (a) and FCC (b) and BCC (c) models

- ***Effective thermal conductivity of simple cubic model:***

The heat flux crossing the simple cubic elementary cell is defined by:

$$Q_{SC} = \int_0^{B+1}\left(\int_0^{Y=X}\left.\frac{dT}{dZ}\right|_{Z=B+1} dY\right)dX \qquad (8)$$

The effective thermal conductivity and the filler volume fraction of the *SC* model are given by:

$$E = 2Q_{SC}/(1+B)\ ;\ \phi_{SC} = \pi/6(1+B)^3$$

- ***Effective thermal conductivity of FCC model (Figure 3):***

The heat flux crossing the face centered cubic elementary cell is defined by:

$$Q_{FCC} = \left[\begin{array}{l}\iint_{S_1}\frac{dT}{dZ}dYdX + \frac{1}{D}\iint_{S_2}\frac{dS}{dZ}dYdX \\ + \frac{1}{D}\iint_{S_3}\frac{dS}{dZ}dYdX_3\end{array}\right] \qquad (9)$$

The effective thermal conductivity and the filler volume fraction of the *FCC* model are given by:

$$E = 2Q_{FCC}/(1+B) \quad \text{and} \quad \phi_{FCC} = 2\pi/3(1+B)^3 \qquad (10)$$

- ***Effective thermal conductivity of BCC model :***

The heat flux for this case is calculated and the effective thermal conductivity is deduced from the following relation: $E = 2Q_{BCC}/(1+B)$. The filler amount ϕ_{BCC} is correlated to B by: $\phi_{BCC} = \pi/3(1+B)^3$, with :

$$Q_{BCC} = \left[\iint_{S_1}\frac{dT}{dZ}dS_1 + \frac{1}{D}\iint_{S_2}\frac{dS}{dZ}dS_2\right] \qquad (11)$$

2.2. Experimental study

In our experimental set-up, the matrix material is an epoxy resin of *VANTICO* Company. The Araldite® LY5052 is mixed to 38% weight of Aradur® 5052. The brass spheres (70%Cu, 30% Zn, $\rho_{brass} = 8530 Kg/m^3$) of 3.18 *mm* and 6.35 *mm* of diameter with a thermal conductivity of 124 $W.m^{-1}K^{-1}$ were placed in aluminum mold cavity ($45\times45 mm^2$). Three samples were prepared under the same conditions: the first two are presented in figures 3 and 4. The first configuration is a simple cubic with brass spheres of 6.35 *mm* diameter and the second one is an hexagonal arrangement, with a maximum volume fraction (14) with brass spheres (3.18 *mm* diameter). The third sample is a stacking of three layers of spheres with a 6.35 *mm* diameter which represents a face centered cubic model for its central part (Figure 5).

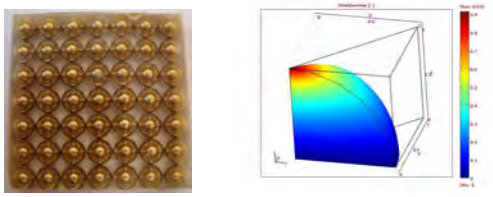

Figure 3: Sample (a) and computed elementary cell

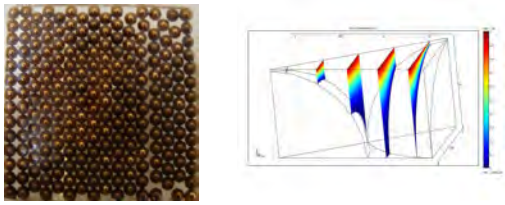

Figure 4: Sample (b), epoxy resin / brass spheres of diameter 3.18mm and computed elementary cell

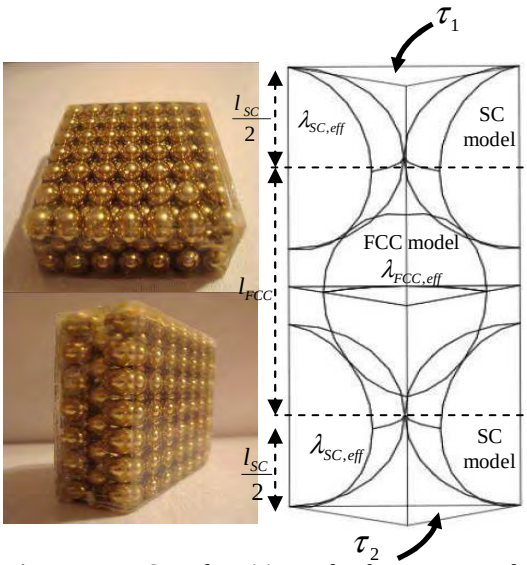

Figure 5: Sample (c) and the computed elementary cell: calculation of the effective thermal conductivity

3. Results and discussion

3.1. Numerical results- effect of filler volume fraction and thermal contact resistance

Thermal conductivity as described in the section 2.1, was computed by the 3D-finite element method, as a function of three quoted parameters *B, C and D*. Computation of about 150 *E* values has showed that a decrease in the contact resistance *C* or of the inner resistance *D* leads to a raise of the effective thermal conductivity. The first set of results for the simple cubic-cell is reported in figure 6. We observe that the lower and the higher limits of simple cubic thermal conductivity *E* are, respectively, 2.30 and 6.28.

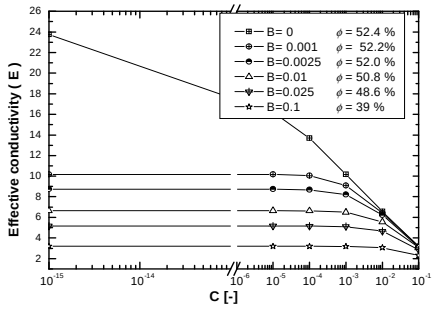

Figure 6: ETC versus C and B, SC model ($D = 10^{-5}$)

Figures 7 and 8 show the variation of the *ETC* for face centered cubic (*FCC*) and body centered cubic (*BCC*) for different contact resistances and filler volume fractions ϕ. Similar behavior can be noted with the SC model. As seen from the figures, for low filler volume fraction $\phi \le 50\%$, the calculated effective conductivities are nearly the same for both *BCC* and *FCC* models. The maximum effective thermal conductivity for both *BCC* and *FCC* models was calculated in the perfect interface case, i.e. no jump temperature across the resin/spheres interface ($E_{BCC} = 6.34$ and $E_{FCC} = 5.97$ respectively).

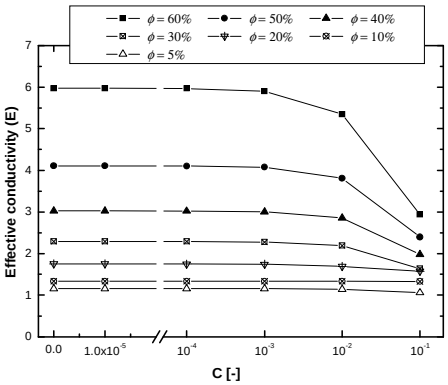

Figure 7: Effect of the thermal contact resistance on the ETC for different filler volume fractions (FCC model, $D = 10^{-5}$).

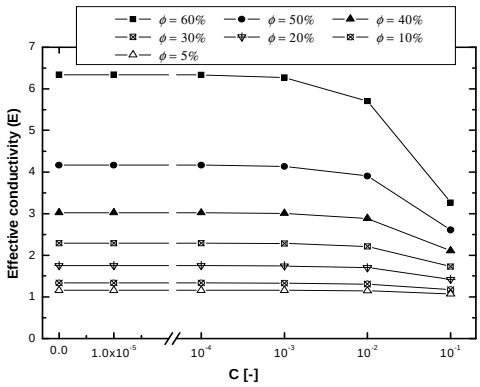

Figure 8: Effect of the thermal contact resistance on the ETC for different filler volume fractions (BCC model, $D = 10^{-5}$)

3.2. Comparison between analytical models and numerical simulations

To illustrate the difference between the numerical and analytical models, we have plotted in figure 9 the *ETC* versus the ratio of the thermal conductivity of filler to the one of the matrix material for a $\phi = 52\%$ volume fraction and $C = 10^{-1}$. Note that as $D = \lambda_m / \lambda_f \geq 10^{-3}$, it appears that both numerically and analytically computed thermal conductivities increase very slightly and tends to a constant value. Therefore, the use of higher conductive filler ($\lambda_f \succ 10^3 W.m^{-1}.K^{-1}$) is not interesting to enhance thermal composite conductivity. Thus, typically brass or aluminum fillers seem to be ideal materials from this point of view. We can observe that the effective conductivities of *FCC* and *BCC* models are fairly close to the Sthrikman model.

The examination of these results shows that the difference between the Sthrikman model and the numericals *ETC* lies between 2.4% and 7.9% for the *SC* model and about 17% for the *BCC* model. On another side, for $D \in \left[10^{-3}, 10^{-1}\right]$, it is interesting to show that the difference between the analytical and the numerical *ETC* decreases from 5% for simple cubic model to the value of 13% of the *BCC* model. The results from our numerical calculation and Lewis & Nielsen model versus filler volume fraction are shown in figure 10 ($D = 10^{-4}, C = 10^{-5}$). It is found that the analytical0 models predicts the same tendency and represents a relatively good agreement with the numerical results and the effective thermal conductivity increases slightly from 1 to 2.29 for $\phi \in [0\% - 30\%]$. This indicates that spheres are dispersed in matrix and they are not interacting with each other. However, a deviation from the numerical results is observed when the percentage of inclusions is larger $\phi \geq 40\%$ and a better agreement is achieved with $\phi_{\max} = 74\%$. On the other hand, for filler volume fraction greater than 30%, the conductive filler cause an exponential increases in the effective thermal conductivity of the composite (for example from 2.29 to 6.34 for *BCC* model).

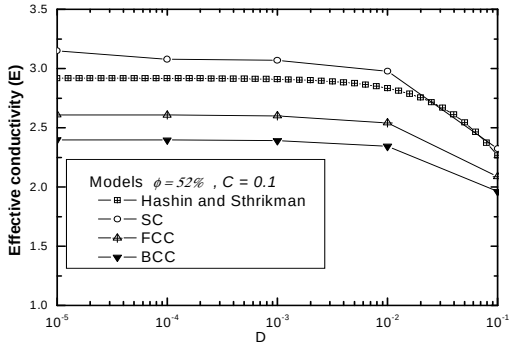

Figure 9: Calculated ETC and Sthrikman prediction versus the inner resistance D (C = 0.1, ϕ= 52%)

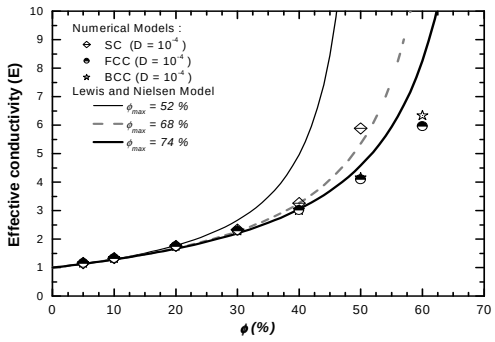

Figure 10: Calculated ETC and Nielsen prediction versus the filler volume fraction ϕ (%), $C = 10^{-5}$

3.3. Comparisons between simulations, analytical model and experimental data

The thermal conductivity and diffusivity of the samples are measured simultaneously by using a so-called periodic method, using multi-harmonic heating signals and inverse problem [19]. The sample (a) is composed of a brass sphere of radius $r = 3.17mm$ centered in parallelipipedic epoxy matrix. Figure 3 shows the calculated elementary cell and the effective thermal conductivity is given by the following equation: $E_{(a)} = 2Q_{SC}(1 + B_{SC,m})$. $B_{SC,m}$ is the measured distance between the sphere and the upper surface divided by the sphere radius. The second sample is an hexagonal arrangement, especially in the central part, figure 4. Hence, based on the

computed dimensionless heat flux on the upper surface of the elementary cell $Q_H = \int_0^{(B+1)\sqrt{3}} \left(\int_0^{Y=X/\sqrt{3}} \left. \frac{dT}{dZ} \right|_{Z=B+1} dY \right) dX$ the effective thermal conductivity can be re-written: $E_{(b)} = 2Q_H(1+B_{H,m})/\sqrt{3}$. The third sample (c) is a stacking of three layers. The upper and the lower layers represent a simple cubic elementary cell with $B_{SC,m} = 0$ and a thickness of $l_{sc}/2 = r$. The medium layer is a face centered cubic elementary cell with $B_{FCC} = 0.455$ and a thickness of $l_{FCC} = 2\sqrt{2}r$ (Figure 5). Hence the effective thermal conductivity of the sample (c) elementary cell is: $E_{(C)} = E_{SC}E_{FCC}l_{(c)}/\left(E_{FCC}l_{sc} + E_{SC}l_{FCC}\right)$ where $E_{SC} = 2Q_{SC}$, $E_{FCC} = 2Q_{FCC}/\left(1+B_{FCC}\right)$ and $l_{(c)} = 2r\left(\sqrt{2}+1\right)$ are the effective thermal conductivities for simple cubic and face centered cubic arrangements and the thickness of the face centered cubic model, respectively. In order to illustrate the difference between the measured effective conductivities, the calculated values from *FEM* simulations E_c and the analytical predictions, we assume the perfect contact between the brass spheres and the epoxy matrix. Figure 11 shows the comparison between the analytical prediction, the calculated values and the measured data of the thermal conductivity of epoxy-resin/brass-spheres composite. It can be seen that the Nielsen values are fairly close to the experimental measured data of *E*. Relatively, the analytical results with $\phi_{\max} = 68\%$ are closer to the experimental measured data of E_m than those with $\phi_{\max} \neq 68\%$. The experimental values E_m at about 20°C are compared to the calculated values E_c from *FEM* simulations. The results show that the difference between E_c and E_m is lower than 2%. It is interesting to note that the parameter B_m plays a fundamental role on the heat transfer between the matrix and spheres and thus influences largely the value of effective thermal conductivity. For the samples (c), the parameter B_m is very low ($B_m \cong 0$) in this case the difference between E_c and E_m is about 1.52%. We can also observe the influence of this parameter on the effective thermal conductivities of the sample (a) and (b). It may be seen that the differences between E_c and E_m decrease when B_m decreases, it means when the volume fraction ϕ increases. Thus, it seems that the variation measurement-models is lower at a weak volume fraction. This indicates that the control of the parameter B_m is significant to measure the effective thermal conductivity and to understand the heat transfer behavior of the composites.

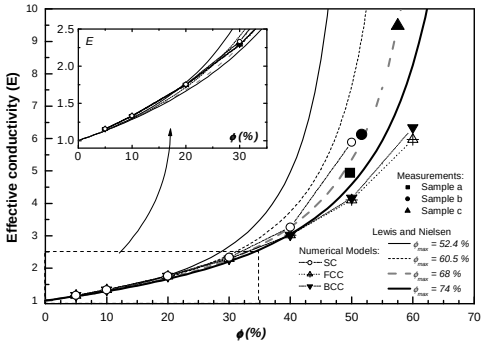

Figure 11: Calculated, measured effective thermal conductivities and Nielsen model versus filler volume fraction ϕ(%). The conductivity ratio between resin matrix and brass spheres: $D = 0.00165$.

4. Conclusions

Prediction of the thermal conductivity of composite materials is crucial in a number of industrial processes. All the theoretical and empirical models fail to predict *ETC* of composites in the whole range of filler content. As seen from this study, Hashin and Sthrikman and Lewis & Nielsen models predict fairly well thermal conductivity values up to 30% by volume of brass spheres whereas beyond 30% of inclusion content, all models underestimate the thermal conductivity of the composite. From the thermal conductivity measurements for three samples of composite at volume fraction from 49% to 57%, it may be concluded that thermal conductivity has increased from 0.2 $W.m^{-1}K^{-1}$ for pure epoxy resin to $1.94 W.m^{-1}K^{-1}$. Furthermore, the measured values were found to

be in good agreement with numerical data, especially for sample (b). The influence of the reduced outer resistance B of the matrix layer between nearest spheres on the *ETC* is presented and trends are discussed. It is shown that B plays a significant role in the composite heat transfer.

5. References

1. Zalba B., Marín J. M., Cabeza L. F., Mehling H., Review on thermal energy storage with phase change: materials, heat transfer analysis and applications, Applied Thermal Engineering. 23 251(2003).
2. Milton G. W., *The theory of composites, Cambridge University Press*, Cambridge, UK; 2002.
3. Furmañski P., Heat conduction in composites: Homogenization and macroscopic behavior, Applied Mechanics Review. 50, 327(1997).
4. Mirmira, S. R., Fletcher L. S., Comparative Study of Thermal Conductivity of Graphite Fiber Organic Matrix Composites, Proceeding of the 5th ASME/JSME Joint Thermal Engineering Conference, San Diego, C. A., Paper A JTE99-6439 (1999).
5. Deissler R. G., Boegli J. S., An Investigation of Effective Thermal Conductivities of Powders in. Various Gases, Trans ASME. 80,1417 (1958)
6. Wakao N., Kato K., Effective thermal conductivity of packed beds, Chemical Engineering of Japan. 2, 24 (1969).
7. Shonnard D. R., Whitaker S., The effective thermal conductivity for a pointcontact porous medium: an experimental study, Int. J. Heat Mass Transfer. 32, 503(1989).
8. Auriault J-L., ENE H. I., Macroscopic modelling of heat transfer in composites with interfacial thermal barrier, Int. J. Heat Mass Transfer, 37, 2885(1994).
9. Veyret D., Cioulachtjian S., Tadrist L., Pantaloni J., Effective Thermal Conductivity of a Composite Material: A Numerical Approach, Journal of Heat Transfer. 115, 866(1993).
10. Ramani K., Vaidyanathan A., Finite Element Analysis of Effective Thermal Conductivity of Filled Polymeric Composites, Journal of Composite Materials. 29, 1725(1995).
11. Cruz ME, *Computational methods and Experimental Measurements* X, WIT Press, Southampton, UK, 657 (2001).
12. Yin Y., Tu S.-T., Thermal Conductivities of PTFE Composites with Random Distributed Graphite Particles, Journal of Reinforced Plastics and Composites. 21, 1619 (2002).
13. Kumlutas D., Tavmana I. H., Coban M. T., Thermal conductivity of particle filled polyethylene composite materials, Journal of Composite Science and Technology. 63, 113 (2003)
14. Jiang M., Ostoja-Starzewski M., Jasiuk I., Apparent thermal conductivity of periodic two-dimensional composite, Journal of the computational Materials Science. 25, 329 (2002).
15. Liang J. Z., Li F. H., Simulation of heat transfer in hollow glass bead filled polypropylene composites by finite element method, Polymer Testing. 26, 419 (2007).
16. Fiedler T., Löffler R., Bernthaler T., Winkler R., Belova I. V., Murch G. E., Öchsner A., Numerical analyses of the thermal conductivity of random hollow sphere structures, Materials Letters, 63, 1125(2009).
17. Fiedler T., Belova I. V., Öchsner A., Murch G. E., Non-linear calculations of transient thermal conduction in composite materials, Computational materials science. 45, 434 (2009).
18. Danes F., Garnier B., Dupuis T., Predicting, Measuring, and Tailoring the Transverse Thermal Conductivity of Composites from Polymer Matrix and Metal Filler, Int. J. Thermophysics. 24, 771(2003).
19. Karkri M., Jarny Y., Mousseau P., Inverse heat transfer analysis in a polymer melt flow within an extrusion die, Inverse Problems in Science and Engineering.13, 355 (2005).